Inorganic Chemistry

Article

pubs.acs.org/IC

A New Series of Chiral Metal Formate Frameworks of $[HONH_3][M^{II}(HCOO)_3]$ (M = Mn, Co, Ni, Zn, and Mg): Synthesis, Structures, and Properties

Bin Liu, Ran Shang, Ke-Li Hu, Zhe-Ming Wang,* and Song Gao*

Beijing National Laboratory for Molecular Sciences, State Key Laboratory of Rare Earth Materials Chemistry and Applications, College of Chemistry and Molecular Engineering, Peking University, Beijing 100871, People's Republic of China

Supporting Information

ABSTRACT: We report the synthesis, crystal structures, IR, and thermal, dielectric, and magnetic properties of a new series of ammonium metal formate frameworks of $[HONH_3][M^{II}(HCOO)_3]$ for M = Mn, Co, Ni, Zn, and Mg. They are isostructural and crystallize in the nonpolar chiral orthorhombic space group $P2_12_12_1$, a = 7.8121(2)−7.6225(2) Å, b = 7.9612(3)−7.7385(2) Å, c = 13.1728(7)−12.7280(4) Å, and V = 819.27(6)−754.95(4) Å^3. The structures possess anionic metal formate frameworks of $4^9{\cdot}6^6$ topology, in which the octahedral metal centers are connected by the anti−anti formate ligands and the hydroxylammonium is located orderly in the channels, forming strong O/N−H···$O_{formate}$ hydrogen bonds with the framework. $HONH_3^+$ with only two non-H atoms favors the formation of the dense chiral $4^9{\cdot}6^6$ frameworks, instead of the less dense $4^{12}{\cdot}6^3$ perovskite frameworks for other monoammoniums of two to four non-H atoms because of its small size and its ability to form strong hydrogen bonding. However, the larger size of $HONH_3^+$ compared to NH_4^+ resulted in simple dielectric properties and no phase transitions. The three magnetic members (Mn, Co, and Ni) display antiferromagnetic long-range ordering of spin canting, at Néel temperatures of 8.8 K (Mn), 10.9 K (Co), and 30.5 K (Ni), respectively, and small spontaneous magnetizations for the Mn and Ni members but large magnetization for the Co member. Thermal and IR spectroscopic properties are also reported.

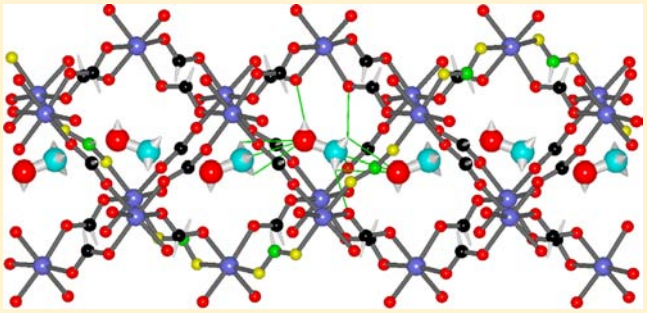

INTRODUCTION

The prosperity and continuing rapid developments in the research of metal−organic frameworks (MOFs) have provided materials showing a very wide spectrum of properties, functionalities, and possible applications, and this field has relevance to almost every aspect of material sciences.[1−8] Indeed, these organic−inorganic hybrids, consisting of inorganic metal ions and organic components as the building blocks, can possess new and interesting properties or functionalities, originating from such inorganic−organic combinations.[2] Porosity, framework dynamics, and reactivity beneficial for catalysis, gas/solvent absorption/storage/separation and even drug delivery,[3] light absorption/emission and chirality for optics,[4] magnetic and electric interactions for magnetism and dielectricity even ferro/antiferroelectricity,[5] and so on, have all been realized within MOFs. Furthermore, the coexistence of two or more properties, or multifunctionalities, within a single phase, for example, magnetic and electric properties,[6] magnetic and optical properties,[7] and porosity and magnetism,[8] could be possible when the related functional building blocks or structural features are incorporated. Such multifunctional materials currently attract considerable attention because they provide a good approach to creating smart materials and devices with dual functionality or multifunctionality and possible interplay between different functions.[6−8,9a]

In this context, we and several other groups have continued to explore and investigate the functional metal formate frameworks templated by protonated amines, and such endeavors have led to many interesting outcomes and achievements.[9−25] The template effect has been clearly revealed by the employment of different sized and structured ammonium cations.[9a] For 3d transition-metal (TM) ions and Mg^{2+}, the small NH_4^+ resulted in chiral frameworks of $[NH_4][M(HCOO)_3]$ with rarely observed $4^9{\cdot}6^6$ topology in which the octahedral metal ions are connected by anti−anti formate and the NH_4^+ cations are located in the channels.[10] The use of monoammonium, $AmineH^+$ = $CH_3NH_3^+$,[11] $(CH_3)_2NH_2^+$,[11a,12] $CH_3CH_2NH_3^+$,[11a] $C(NH_2)_3^+$,[13] and $(CH_2)_3NH_2^+$,[11a,14] and very recently reported $(NH_2)_2CH^+$,[15] with two to four non-H atoms, has resulted in many series of metal formate perovskites of $[AmineH^+][M(HCOO)_3^-]$, possessing frameworks of $4^{12}{\cdot}6^3$ topology, in which the metal−metal linkages are also via anti−anti formates and the ammonium cations sit in the framework cavities. The more

Received: October 1, 2012
Published: December 5, 2012

Table 1. Crystallographic Data for 1Mn, 2Co, 3Ni, 4Zn, and 5Mg

	1Mn	2Co	3Ni	4Zn	5Mg
ionic radius of M^{2+}, Å	0.97	0.89	0.83	0.88	0.86
formula	$C_3H_7MnNO_7$	$C_3H_7CoNO_7$	$C_3H_7NiNO_7$	$C_3H_7ZnNO_7$	$C_3H_7MgNO_7$
fw	224.04	228.03	227.81	234.47	193.41
T, K	293	293	293	293	293
crystal system	orthorhombic	orthorhombic	orthorhombic	orthorhombic	orthorhombic
space group	$P\,2_12_12_1$	$P\,2_12_12_1$	$P\,2_12_12_1$	$P\,2_12_12_1$	$P\,2_12_12_1$
a, Å	7.8121(2)	7.6839(3)	7.6225(2)	7.6892(2)	7.6883(2)
b, Å	7.9612(3)	7.7555(3)	7.7814(4)	7.7385(2)	7.7875(2)
c, Å	13.1728(7)	13.0195(6)	12.7280(4)	13.0205(4)	12.8558(4)
α, deg	90	90	90	90	90
β, deg	90	90	90	90	90
γ, deg	90	90	90	90	90
V, Å^3	819.27(6)	775.86(6)	754.95(4)	774.76(4)	769.71(4)
Z, D_c, g/cm^3	4, 1.816	4, 1.952	4, 2.004	4, 2.010	4, 1.669
μ(Mo Kα), mm^{-1}	1.614	2.215	2.573	3.173	0.234
F(000)	452	460	464	472	400
crystal size, mm^3	0.12 × 0.12 × 0.10	0.15 × 0.15 × 0.13	0.08 × 0.07 × 0.05	0.42 × 0.42 × 0.32	0.28 × 0.23 × 0.20
T_{min}, T_{max}	0.783, 0.859	0.688, 0.756	0.806, 0.889	0.318, 0.375	0.893, 0.956
θ_{min}, θ_{max}, deg	3.65, 27.48	3.73, 27.46	3.74, 27.45	3.74, 27.51	3.72, 27.50
no. of total reflns	13823	14052	15478	14875	12604
no. of unique reflns (R_{int})	1876 (0.0590)	1763 (0.0731)	1725 (0.0787)	1770 (0.0481)	1750 (0.0453)
no. of obsd reflns [$I \geq 2\sigma(I)$]	1401	1283	1409	1602	1583
no. of param	110	109	109	110	110
Flack parameters	0.65(2)	0.01(2)	0.00(2)	−0.01(1)	0.9(2)
R1,[a] wR2[b] [$I \geq 2\sigma(I)$]	0.0267, 0.0487	0.0301, 0.0543	0.0302, 0.0597	0.0190, 0.0445	0.0263, 0.0722
R1,[a] wR2[b] (all data)	0.0470, 0.0513	0.0561, 0.0580	0.0435, 0.0623	0.0233, 0.0454	0.0314, 0.0741
GOF	0.919	0.947	0.987	0.991	1.137
$\Delta\rho$,[c] e/Å^3	0.313, −0.212	0.483, −0.308	0.434, −0.502	0.270, −0.417	0.182, −0.217
max, mean Δ/σ[d]	0.000, 0.000	0.001, 0.000	0.000, 0.000	0.001, 0.000	0.000, 0.000

[a] $R1 = \sum||F_o| - |F_c||/\sum|F_o|$. [b] $wR2 = [\sum w(F_o^2 - F_c^2)^2]/\sum w(F_o^2)^2]^{1/2}$. [c] Maximum and minimum residual electron density. [d] Maximum and mean σ/shift.

bulky AmineH$^+$ cations such as $(CH_3CH_2)_3NH^+$, however, acted as negative templates and led to formation of the porous family of $[M_3(HCOO)_6]$[16−21] with diamond topology where formate adopts a syn−syn/anti mode. When the protonated linear di-, tri-, and tetraamines were employed, novel binodal metal formate frameworks of $(4^{12}\cdot6^3)(4^9\cdot6^6)_n$ for n = 1−3, could be obtained.[9a,22,23] Among them, the longer cationic templates directed the formation of longer framework cavities, and the series[23] with $(4^{12}\cdot6^3)(4^9\cdot6^6)$ topology (n = 1) represented the first metal−organic analogous to the minerals niccolite (NiAs) or colquiriite ($LiCaAlF_6$). The studies have been very recently expanded into lanthanides (Ln); various lanthanide formate frameworks with more complicated topologies could be synthesized, even using the simple monoammonium templates, and this is due to the higher variability of Ln ions in coordination.[24] These works revealed not only the benefit of formate for the formation of extended structures, and thus MOFs, but also the significant malleability and adaptability of these metal formate frameworks to conform to the templates.[9a,b] As (magnetic) metal ions, short formato bridges, and ammonium cations/polar solvents are incorporated, and the later components are beneficial for hydrogen-bonding, these materials exhibit promising magnetic, dielectric, porous, and optical properties and possible multifunctionality. The porous $[M_3(HCOO)_6]$ family showed a wide spectrum of guest-inclusion[16−21] and guest-dependent magnetism.[9c,16a,b,17,18,21] Many magnetic ammonium transition-metal formates are spin-canted antiferromagnets or weak ferromagnets (hereafter we use AF as the abbreviation for antiferromagnet/antiferromagnetism/antiferromagnetic, and WF for weak ferromagnets/weak ferromagnetism), and the critical temperatures can be as high as 35 K.[9a,b,10−13] The coexistence or synergism of magnetic and electric orderings has been documented for magnetic members of $[NH_4][M(HCOO)_3]$[10] and $[(CH_3)_2NH_2][M(HCOO)_3]$[12] series and $[Mn_3(HCOO)_6]$(polar solvent),[21] affording a new class of molecule-based multiferroics.[26] Giant dielectric constant and dielectric relaxor behaviors have been observed for $[(CH_2)_3NH_2][M(HCOO)_3]$.[14] Magnetic relaxation behaviors and structural transitions have been reported for several lanthanide formate systems.[24] Negative expansion upon increased pressure and cooling has been observed for $[NH_4][TM(HCOO)_3]$.[10a,b,h] Chiral $[NH_4][M(HCOO)_3]$[10] and $[AmineH][Ln(HCOO)_4]$[24b,c] solids represented interesting examples of the emergence of chirality during crystallization from the achiral components. Finally, mixed-valent and mixed-metal systems added new possibilities,[9c,10d−f,11b,25] such as magnetic dilution and metal-component-modulated phase-transition temperatures. All of these indicate that the metal formate frameworks, while being a small class of MOFs, provide us new opportunities to create novel materials with interesting properties.

To continue our research on metal formates, in this work we use hydroxylammonium ($HONH_3^+$) as the template cation to construct a new series of $[HONH_3][M^{II}(HCOO)_3]$ compounds, namely, **1Mn**, **2Co**, **3Ni**, **4Zn**, and **5Mg** for M = Mn,

Co, Ni, Zn, and Mg, respectively. The $HONH_3^+$ cation is simple and has two non-H atoms, larger than NH_4^+, and it led to the formation of the chiral frameworks with $4^9{\cdot}6^6$ topology and chirality from simple achiral reactants. The synthesis, structures, template role of $HONH_3^+$, dielectric, thermal, and IR properties, and magnetism for the magnetic members have been investigated, and the detailed results are reported here.

EXPERIMENTAL SECTION

Synthesis. All chemicals, reagent grade, were commercially available and were used without further purification. The compounds reported in this work were prepared under aerobic conditions. ***Caution!*** *Perchlorate compounds are potentially explosive. They should be used in small quantities and handled with care.*

The compounds of the $[HONH_3][M^{II}(HCOO)_3]$ series were synthesized by very similar methods. The preparation of **1Mn** is described as an example. A 10 mL methanol solution containing 3.94 g (80 mmol) of formic acid, 1.06 g (10.0 mmol) of triethylamine, and 1.17 g (4.0 mmol) of hydroxylamine hydrochloride was mixed with 5 mL of a methanol solution containing 0.78 g (2.0 mmol) of $Mn(ClO_4)_2{\cdot}6H_2O$. The mixed solution was kept undisturbed. The block-shaped colorless crystals were collected after 1 day, washed with ethanol, and air-dried. Yield: 47%. **2Co**, **3Ni**, **4Zn**, and **5Mg** were obtained after 1 or 2 days of crystallization in yields of 65%, 34%, 56%, and 49%, respectively. To obtain X-ray-quality crystals of **3Ni** of large enough size, the crystallization lasted for 10 days, but the bulk products contained a minor impurity of the porous $[Ni_3(HCOO)_6]{\cdot}S$ (S = solvent), and this issue will be discussed later. Anal. Calcd for $C_3H_7MnNO_7$ (**1Mn**): C, 16.08; H, 3.13; N, 6.25. Found: C, 16.07; H, 3.19; N, 6.31. Calcd for $C_3H_7CoNO_7$ (**2Co**): C, 15.81; H, 3.07; N, 6.14. Found: C, 15.98; H, 3.19; N, 6.13. Calcd for $C_3H_7NiNO_7$ (**3Ni**): C, 15.82; H, 3.07; N, 6.15. Found: C, 16.10; H, 3.32; N, 6.05. Calcd for $C_3H_7ZnNO_7$ (**4Zn**): C, 15.37; H, 3.01; N, 5.97. Found: C, 15.48; H, 3.12; N, 6.14. Calcd for $C_3H_7MgNO_7$ (**5Mg**): C, 18.64; H, 3.62; N, 7.24. Found: C, 18.81; H, 3.71; N, 7.34.

X-ray Crystallography. The crystallographic data for single crystals of the five isostructural compounds were collected at room temperature on a Nonius Kappa CCD diffractometer with a 2.0 kW sealed anode source using graphite-monochromated Mo Kα radiation (λ = 0.71073 Å).[27] The structure of **2Co** was solved first by direct methods and refined, and its structure was used as a starting model for the other compounds. All structures were refined by full-matrix least squares on F^2. The H atoms could be located by difference Fourier syntheses but were added according to the ideal geometries and not refined. The nearly zero Flack parameters[28] for the crystals of **2Co**, **3Ni**, and **4Zn** used in X-ray diffraction indicated their chirality purity, but the crystals of **1Mn** and **5Mg** showed twinning. We kept the same chirality for the structures of **1Mn** and **5Mg** as that for **2Co**, **3Ni**, and **4Zn**, regardless of which handedness was the major domain, by keeping the Flack parameters larger than 0.5. All structural calculations were performed using the *SHELX* program.[29] The data collection, reduction, and crystallographic data are summarized in Table 1. CCDC 909958 (**1Mn**), CCDC 909959 (**2Co**), CCDC 909960 (**3Ni**), CCDC 909961 (**4Zn**), and CCDC 909962 (**5Mg**) contain the supplementary crystallographic data for this paper. These data can be obtained free of charge via www.ccdc.cam.ac.uk/conts/retrieving.html (or from the Cambridge Crystallographic Data Centre, 12 Union Road, Cambridge CB2 1EZ, U.K.; fax (+44) 1223-336-033 or e-mail deposit@ccdc.cam.ac.uk).

Powder X-ray diffraction (PXRD) patterns were collected in the range of $6° < 2\theta < 60°$ at room temperature for bulk samples on a Rigaku Dmax 2000 diffractometer with Cu Kα radiation in a flat plate geometry and for pressed tablet samples on an Agilent Technologies SuperNova Atlas CCD diffractometer with Cu Kα radiation.

Physical Measurements. Elemental analyses of carbon, hydrogen, and nitrogen were performed on an Elementar Vario MICRO CUBE analyzer. Fourier transform infrared spectra were recorded for pure samples in the range of 4000−600 cm^{-1} on a Nicolet iN10 MX spectrometer. Thermal analyses above room temperature were performed on a TA SDT Q600 simultaneous differential scanning calorimetry (DSC)−thermal gravimetry analysis (TGA) instrument at a rate of 5 °C/min under an air atmosphere. DSC in range of −80 to +40−110 °C (depending on sample) was carried out on a TA Q100 instrument at 5 °C/min under a nitrogen atmosphere with two or three cycles.

The temperature-dependent alternating-current (ac) dielectric permittivity measurements were carried out on a TH2828 Precision LCR meter under different frequencies and an applied voltage of 1.0 V under a nitrogen flow. The data were collected at a temperature sweeping rate of 1 °C/min using a homemade temperature-control system. Samples were ground and pressed into tablets under a pressure of ca. 2 GPa, and for **1Mn** to **4Zn**, the phase purity of the pressed tablets and the absence of pressure-induced phase transitions were confirmed by PXRD. The capacitors were made by painting the two faces of the carefully cut tablet pieces with silver conducting paste and gold wires of 40 μm diameter as the electrodes. These capacitors were kept vacuum-dried over silica gel for more than 10 days and then finally coated by a very thin layer of paraffin liquid or AB glue before dielectric measurements, in order to avoid the influence of moisture. The area and thickness of the capacitors were measured under a microscope with a Phenix CCD eye and software. Dielectric measurements could only be performed with a cooling procedure, starting from ca. 30 or 40 °C. When the capacitor cracked, indicated by a sudden drop of the dielectric constant, the measurement was ended.

Magnetic susceptibility measurements, zero-field ac magnetic susceptibility measurements, and the field dependence of magnetization were carried out for the magnetic members **1Mn**, **2Co**, and **3Ni** on a Quantum Design MPMS XL-5 SQUID system for polycrystalline samples tightly packed and sealed in a capsule. All magnetic data had been corrected for the sample diamagnetic susceptibility estimated from Pascal's constants[30] (-87×10^{-6}, -85×10^{-6}, and -83×10^{-6} cm^3/mol for **1Mn**, **2Co**, and **3Ni**, respectively) and background correction by experimental measurement on sample holders.

RESULTS AND DISCUSSION

Synthesis, PXRD, IR Spectra, and Thermal and Dielectric Properties. Our previously works[9] have revealed that the metal formate frameworks templated by ammoniums could be easily prepared by mild solution methods at ambient temperature, in which suitable metal salts and templating amines protonated by formic acid were employed. The preparation of the compounds of the present series followed the same method (see the Experimental Section). However, because the template agent, $HONH_2{\cdot}HCl$, is acidic, triethylamine was added to neutralize formic acid. It has been proven that triethylammonium was a negative template in such reaction systems.[9a] The bulky ammonium, in fact, led to the extensively investigated porous diamond frameworks of $[M_3(HCOO)_6]$ (M = Mn, Fe, Co, Ni, Zn, and Mg) without ammonium in the structures.[16−21] In the present case, the coexistence of bulky triethylammonium and small hydroxylammonium in the reaction system resulted in products of the present series only. This demonstrates the positive templating effect of the small ammoniums.

For the products all harvested after 1 or 2 days of crystallization, the experimental PXRD patterns matched well with the calculated ones based on the single-crystal structures (Figure S1 in the Supporting Information), confirming the phase purity of the bulk samples. For the product of **3Ni**, harvested after 10 days in order to obtain X-ray-quality crystals of a large enough size, the experimental PXRD pattern (Figure S2a in the Supporting Information) of the bulk sample showed several weak peaks corresponding to a small amount of $[Ni_3(HCOO)_6]{\cdot}S$.[9c] To investigate when the impurities formed, crystallization was performed again, and the crystalline

dx.doi.org/10.1021/ic302129m | Inorg. Chem. 2012, 51, 13363−13372

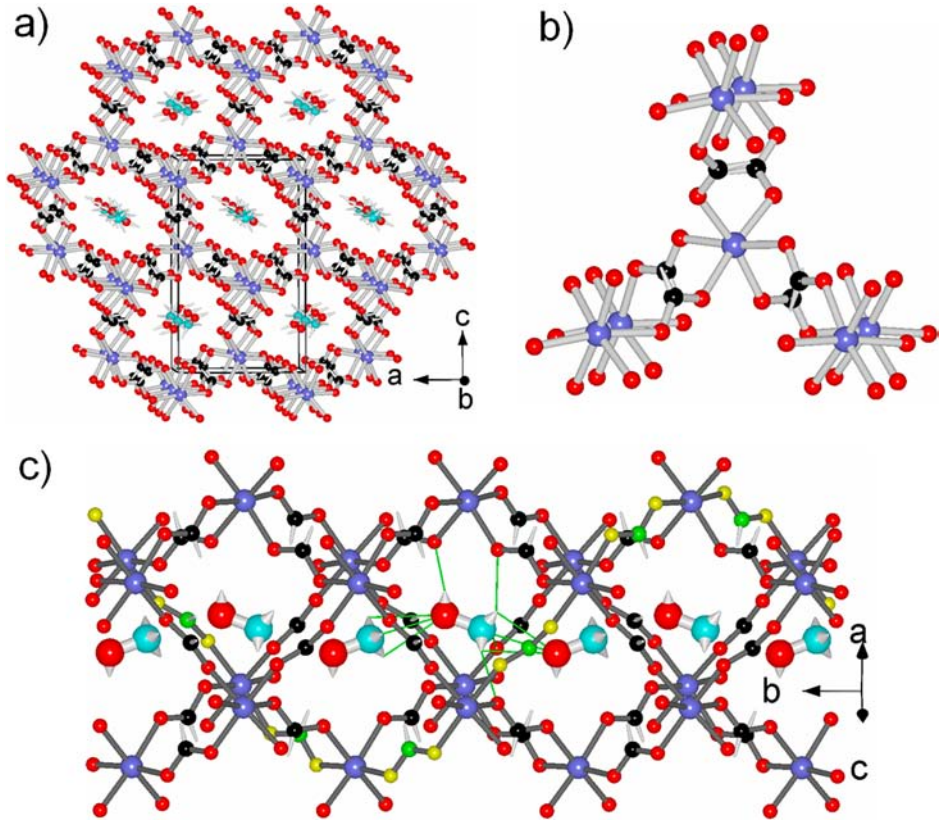

Figure 1. Structure of $[HONH_3][M(HCOO)_3]$, taking **3Ni** as a representative. (a) 3D view of the chiral $4^9{\cdot}6^6$ framework structure viewed down the *b* axis. (b) Local environment around one metal site and its neighboring six metal sites arranged in a trigonal prism. (c) Side view of one framework channel, with the $HONH_3^+$ cations highlighted in large spheres and thick bonds, and one helix of ···Ni−OCHO−Ni−OCHO··· with HCOO bridges in yellow (O) and green (C). Atomic scheme: purple, Ni; black/green, C; red/yellow, O; cyan, N; white, H. The green thin bonds in part c are N/O−H···$O_{formato}$ hydrogen bonds and the possible NH_3···O−H pseudo ones.

products were harvested at different times over 10 days of crystallization and the solid products subjected to PXRD examination. As shown in Figure S2a in the Supporting Information, the peaks corresponding to the impurity phase started to appear from the sixth day and became slightly more perceivable later. The formation of the $[Ni_3(HCOO)_6]{\cdot}S$ phase could be due to its very low solubility.[9c] While the amount of impurity was small in the product of **3Ni** harvested after 10 days of crystallization, it did contribute to the magnetism (Figure S2b in the Supporting Information; see the discussion about magnetism later). We therefore characterized the product of **3Ni** harvested after 2 days of crystallization, which was proven to be phase-pure by PXRD (Figure S1 in the Supporting Information).

Finally, attempts to prepare the Fe and Cu members within this series were not success, probably because of the oxidation (Fe^{II} to Fe^{III}, by air) and reduction (Cu^{II} to Cu^{I}, by NH_2OH) occurring during the preparation and details not discussed further.

The IR spectra of the five compounds are almost the same (Figure S3 in the Supporting Information), as expected given the fact that they are isostructural, and quite similar to those of previously reported ammonium metal formates.[10c,11,13a,22−24] Assignments of the absorption bands are listed in Table S1 in the Supporting Information. These bands are characteristic of the formate and $HONH_3^+$.[31,32] The medium broad bands for N/O−H stretching in 3400−3000 cm^{-1} have lower frequencies than the free ones, indicating the formation of hydrogen bonding involving these groups. $-NH_3^+$ overtones around 2500 cm^{-1}, N−H bending around 1660 and 1530 cm^{-1}, $-NH_2$ rocking (possible) around 1250 cm^{-1}, and O−H bending around 1200 cm^{-1} were observed. Strong bands for the $HCOO^-$ group around 1600, 1580, 1380, and 1360 cm^{-1} probably include bands for N−H bending. Most bands for **3Ni** have the highest or lowest frequency values within the series.

The thermal stability and decomposition behaviors for the five compounds were investigated by combined TGA−DSC experiments performed under an air atmosphere (Figure S4 in the Supporting Information). The materials all showed two clearly separated steps of thermal processes. The first endothermic decompositions occurred around 140, 180, 200, 130, and 180 °C for **1Mn**, **2Co**, **3Ni**, **4Zn**, and **5Mg**, respectively, and the weight losses were 35.5, 36.8, 37.1, 33.8, and 40.8%, respectively, corresponding to the departure of one $NH_2OH{\cdot}HCOOH$ per formula with the calculated weight losses of 35.3, 34.7, 34.7, 33.7, and 40.9%. The intermediate $M(HCOO)_2$ phases further decomposed around 280 °C for **1Mn**, **2Co**, and **3Ni**, 210 °C but lasted to ca. 500 °C for **4Zn**, and 430 °C for **5Mg**. After pyrolysis, the final residues at 800 °C were 33.4, 35.4, 34.4, 34.5, and 24.6% for **1Mn**, **2Co**, **3Ni**, **4Zn**, and **5Mg**, respectively, which are basically in agreement with the calculated values of 31.7, 32.9, 32.8, 34.7, and 20.8% based on the MO oxides, although the slightly higher experimental residues might indicate the possible existence of small amounts of Mn_2O_3, Co_2O_3, and $MgCO_3$. It should be mentioned that thermal decomposition of **4Zn** was seemingly more complicated, as indicated by the DSC trace in which a strong exothermic peak appeared at the end of the first

dx.doi.org/10.1021/ic302129m | *Inorg. Chem.* 2012, 51, 13363−13372

Table 2. Selected Bond Distances (Å) and Bond Angles (deg), Geometries of the N/O−H···O Hydrogen Bonds (N/O···O Distances, Å, and N/O−H···O Angles, deg), and M···M Distances (Å) in 1Mn, 2Co, 3Ni, 4Zn, and 5Mg[a]

	1Mn	2Co	3Ni	4Zn	5Mg
M−O(1)	2.195(2)	2.104(2)	2.058(2)	2.116(1)	2.097(1)
M−O(2)$^{\#1}$	2.235(2)	2.153(2)	2.061(2)	2.173(1)	2.132(1)
M−O(3)	2.164(2)	2.082(2)	2.066(2)	2.085(2)	2.067(1)
M−O(4)$^{\#2}$	2.160(2)	2.081(2)	2.061(2)	2.076(1)	2.059(1)
M−O(5)	2.160(2)	2.087(2)	2.052(2)	2.098(2)	2.071(1)
M−O(6)$^{\#3}$	2.149(2)	2.064(2)	2.051(2)	2.061(1)	2.060(1)
C−O	1.215(3)−1.255(3)	1.223(4)−1.260(4)	1.239(4)−1.260(4)	1.226(3)−1.261(3)	1.233(2)−1.255(2)
N−O	1.405(3)	1.399(3)	1.385(4)	1.394(2)	1.396(2)
cis-O−M−O	79.87(6)−97.17(6)	80.71(8)−94.72(8)	80.81(8)−95.39(8)	80.02(6)−95.77(6)	81.68(5)−94.95(5)
trans-O−M−O	167.58(6)−173.80(7)	170.28(8)−173.97(9)	170.63(8)−174.03(9)	168.80(6)−174.26(6)	170.55(5)−175.90(5)
M−O−C	115.6(2)−129.4(2)	116.4(2)−129.1(2)	121.3(2)−129.8(2)	116.3(1)−128.9(2)	117.1(1)−131.6(1)
O−C−O	125.7(2)−128.3(2)	125.6(3)−126.1(3)	123.7(3)−125.4(3)	124.7(2)−125.1(2)	125.3(2)−127.2(2)
N−H···O_{HCOO}	2.999(3), 159.1	3.031(3), 159.5	2.943(4), 140.0	3.023(2), 159.8	3.025(2), 159.2
	2.792(3), 164.2	2.801(4), 162.3	2.829(4), 161.8	2.796(2), 162.6	2.798(2), 163.5
	2.889(2), 168.5	2.896(3), 165.9	3.036(4), 163.1	2.894(2), 164.3	2.897(2), 166.5
N−H···O_{OH}	2.882(3),	2.798(3),	2.743(4),	2.803(2),	2.830(2),
	96.4−107.8	96.5−106.5	88.6−100.2	96.8−106.7	97.0−106.3
O−H···O_{HCOO}	2.678(2), 162.3	2.687(3), 161.3	2.621(3), 146.2	2.674(2), 162.0	2.680(2), 162.3
	3.054(2), 121.0	2.947(3), 122.2	3.084(3), 129.7	2.939(2), 120.2	2.980(2), 121.6
M···M	5.945 × 2	5.833 × 2	5.747 × 2	5.815 × 2	5.827 × 2
	5.957 × 2	5.843 × 2	5.833 × 2	5.855 × 2	5.829 × 2
	6.071 × 2	5.944 × 2	5.903 × 2	5.939 × 2	5.945 × 2

[a]Symmetry codes: #1, $-x + 1, y + {}^1/_2, -z + {}^1/_2$; #2, $x + {}^1/_2, -y + {}^1/_2, -z$, #3, $x + {}^1/_2, -y + {}^3/_2, -z$.

endothermic step and also a lasting pyrolysis with several, broadened exothermic peaks. The thermal stability of this series is similar to that of other [AmineH][M(HCOO)$_3$] compounds.[10,11,22−24]

The DSC measurements (Figure S5a in the Supporting Information) revealed the absence of phase transition in the temperature range investigated for the five compounds. Dielectric studies showed that no dielectric anomalies were observed for **1Mn** to **4Zn** below 30 or 40 °C, and dielectric constants (ε' at 1 MHz; Figure S5b in the Supporting Information) were in the range of 5−8. These low ε' values are in agreement with the nonpolar, ordered structures discussed below, and the series is different from the recently reported ferroelectric series of [NH$_4$][M(HCOO)$_3$],[10] although the framework structures are quite similar. The pressed tablet sample of **5Mg** was observed to possess a PXRD pattern (not given here) different from that of the as-prepared sample. Currently, it is not clear if pressure-induced phase transition[10h] occurred for **5Mg**, and this merits further investigation.

Crystal Structures. The compounds of this series are isostructural, as observed in many other metal formate series.[9−25] They belong to the chiral but nonpolar orthorhombic space group $P2_12_12_1$ (Table 1). As a representative, the structure of **3Ni** is first described (Figure 1), followed the structure evolution along the series and the templating effect of $HONH_3^+$. The structure of **3Ni** possesses a 3D anionic [Ni(HCOO)$^{3-}$] chiral framework of $4^9{\cdot}6^6$ topology and hydroxylammonium cations located in the framework channels (Figure 1a). To the best of our knowledge, the MOFs with $4^9{\cdot}6^6$ topology are still rare, but this series joins the [NH$_4$][M(HCOO)$_3$],[10] K[M(HCOO)$_3$],[33] and Ln(HCOO)$_3{\cdot}$2H$_2$O families.[34] In the network, the 6-connected octahedral Ni nodes are linked by anti−anti formate, and each unique metal node has six adjacent metal sites arranged in a trigonal prism (Figure 1b). This is different from the octahedral spatial arrangement around metal sites for the perovskite ammonium metal formates.[9a,11−15] The NiO_6 octahedron has Ni−O distances of 2.051(2)−2.066(2) Å, *cis*-O−Ni−O angles of 80.81(8)−95.39(8)°, and *trans*-O−Ni−O angles of 170.63(8)−174.03(9)° (Table 2). These are comparable to other nickel formate compounds. The framework, although not as regular as those in [NH$_4$][M(HCOO)$_3$][10] and K[M(HCOO)$_3$][33] in hexagonal $P6_322$, possesses slightly compressed hexagonal chiral channels (Figure 1a) running along the *b* direction, and the channel's wall is made by a bidirectional triple helix of ···Ni−OCHO−Ni−OCHO··· (Figure 1c). In the channel, the $HONH_3^+$ ions are arranged, head to tail, in a zigzag style. Each O/N−H donor forms a pair of O/N−H···O_{HCOO}, one short and one long, to the anionic metal formate framework. The hydrogen-bonding geometries are N/O···O distances of 2.62−2.80 (short)/2.89−3.08 (long) Å, indicating different hydrogen-bonding strengths, and N/O−H···O angles of 130−169° (Table 2). It is noted that the $HONH_3^+$ ions in the zigzag array have close NH_3···OH contacts between the adjacent cations, with a N···O distance of 2.74 Å and N−H···O angles of 89−100°, and the NH_3 end points to the intermediate region of the two long pair electrons of the OH end. However, this kind of contact might not be a real hydrogen bonding but a pseudo one if we consider that it is between two $HONH_3^+$ cations and the positive charge is dislocalized, like that between two anions, for example, between $HC_2O_4^-$ anions in K[HC_2O_4].[35] That is, the arrangement and orientation of the $HONH_3^+$ cations here probably minimize the intercation repulsion, and this merits further investigation. The formate-bridged Ni···Ni distances are 5.747−5.903 Å, and the framework space provided for each $HONH_3^+$ is 29.6 Å^3, calculated by *PLATON*.[36] As observed in other isostructural metal formate series, the members of the present series show systematic increases in the lattice dimensions, interatomic distances of M−O and M···M, from **3Ni** to **1Mn**, with those

dx.doi.org/10.1021/ic302129m | Inorg. Chem. 2012, 51, 13363−13372

data for **4Zn** and **5Mg** close to those for **2Co**, and these are in good agreement with the increased ionic radii from Ni^{2+} to Mn^{2+}.[37] At the same time, C−O distances slightly shorten and N−O and N···O contacts between $HONH_3^+$ cations slightly expand; however, the geometries of N−H···O_{HCOO} hydrogen bonds do not changed regularly. The cell volumes increase from 755.0 Å^3 for **3Ni** to 819.3 Å^3 for **1Mn**, and the framework volumes for the accommodation of one $HONH_3^+$ change from 29.6 Å^3 of **3Ni**, the smallest, to 34.1 Å^3 of **1Mn**, the largest.

The templating effect of $HONH_3^+$, compared to other monoammoniums, should merit further discussion. The cation has two non-H atoms; however, it led to the $4^9{\cdot}6^6$ metal formate frameworks. This was not expected because the previous works[11−15] reported that the monoammonium templates with two to four non-H atoms, including $CH_3NH_3^+$, $(NH_2)_2CH^+$, $(CH_3)_2NH_2^+$, $CH_3CH_2NH_3^+$, $(CH_2)_3NH_2^+$, and $C(NH_2)_3^+$, resulted in the $4^{12}{\cdot}6^3$ perovskite frameworks, while the cationic templates of one non-H atom like K^+, Cs^+, and NH_4^+ produced the $4^9{\cdot}6^6$ frameworks.[10,33] The van der Waals volumes of NH_4^+, $HONH_3^+$, and $CH_3NH_3^+$ were estimated as 25, 38, and 53 Å^3, respectively, by *PCMODEL 9.1*,[38] and these seemly match the void space volumes, 29−32 Å^3 (Ni to Mn for the $[NH_4][M(HCOO)_3]$ series[10]), 30−34 Å^3 (Ni to Mn for the present series), and 52−57 Å^3 (Zn to Mn for $[CH_3NH_3][M(HCOO)_3]$ series[11]), in which the frameworks could provide for the template cations for known compounds. The packing coefficients[39] of the frameworks of the NH_4^+, $HONH_3^+$, and $CH_3NH_3^+$ series, taking the Mn compounds as representatives, are 0.590, 0.567, and 0.549, respectively (these data for other known manganese(II) formate perovskite frameworks are 0.522−0.493), indicating that the perovskite $4^{12}{\cdot}6^3$ frameworks are less dense than the $4^9{\cdot}6^6$ frameworks, thus allowing the accommodation of larger cationic templates. These data shown here clearly reveal the size effect of the templates. The ability for $HONH_3^+$ to form stronger hydrogen bonds to the metal formate framework than $CH_3NH_3^+$ could also favor the formation of more compact $4^9{\cdot}6^6$ frameworks. The relative size between the cation and framework void space should be a critical factor if the materials will undergo phase transition. For example, the present $[HONH_3][M(HCOO)_3]$, with the cation size equal or slightly larger than the framework void space, showed no phase transition as just discussed, compared to the $[NH_4][M(HCOO)_3]$ series,[10] possessing a cation size smaller than the framework void space at room temperature and undergoing phase transitions in the low-temperature region. Finally, the present series, together with the $[NH_4][M(HCOO)_3]$[10] and $A[M(HCOO)_3]$ (A = alkali-metal ions) ones,[33] provides good examples for the chirality creation in solids from achiral components, and they are of interest for further magnetooptical study.[7a−c,10c]

Before we conclude this part, it should be mentioned that ammonium magnesium formate framework compounds are still rare,[12f,g,15,20] though the transition-metal formates have been studied quite extensively. Mg^{2+} possesses an ionic radius and bonding character similar to those of TM^{2+} ions,[37] and the light magnesium formate framework compounds merit exploration.

Magnetic Properties. The magnetic properties of the three magnetic members **1Mn**, **2Co**, and **3Ni** were investigated using the polycrystalline samples, and their characteristic magnetic data are summarized in Table 3. The three materials are 3D AFs showing WF at low temperature, with small spontaneous magnetization for **1Mn** and **3Ni** but quite large magnetization for **2Co** (Figures 2−4 and S6 in the Supporting Information).

Table 3. Summary of the Magnetic Properties of 1Mn, 2Co, and 3Ni, Curie Constants, Weiss Constants, Listed χT Values, and *g* Factors Based upon the Susceptibility Data under 100 Oe Field (and 10 kOe Data in Parentheses)

	1Mn	2Co	3Ni
C/(cm^3·K/mol)[a]	4.64 (4.50)	3.84 (3.77)	1.48 (1.42)
Θ/K[b]	−14.3 (−13.7)	−56.1 (−54.4)	−73.4 (−67.3)
$(\chi T)_{300\ K}$/(cm^3·K/mol)	4.42 (4.31)	3.21 (3.18)	1.20 (1.16)
$(\chi T)_{min}$/(cm^3·K/mol),[c] T_{min}/K	1.58, 9.0	1.04, 15 (1.03, 15)	0.41, 31.6
$(\chi T)_{max}$/(cm^3·K/mol),[c] T_{max}/K	1.69, 8.5	69.3, 9 (1.32, 10)	2.49, 24.0
$(\chi T)_{2\ K}$/(cm^3·K/mol)	0.43 (0.35)	18.61 (0.29)	0.27 (0.022)
T_N/K[d]	8.8	10.9	30.5, 30.0
T_p/K[e]	8.7	10.8	30.5
		10.0	
H_C/kOe (at 2 K)[f]	0.03	0.06	1
M_R/Nβ (at 2 K)[g]	0.0008	0.11	0.002
$M_{50\ kOe}$/Nβ (at 2 K)	1.56	0.66	0.090
α/deg[h]	0.0008	1.5	0.05
H_{SP}/kOe (at 2 K)[i]	2.0	38	>40
g factor[j]	2.06 (2.03)	2.86 (2.83)	2.43 (2.38)
(J/k_B)/K[k]	−0.40	−3.6	−9.2

[a]Curie constants. [b]Weiss constants. [c]Minimum and maximum χT values and the related temperatures. [d]Critical temperatures based on ZFC/FC measurements. For **3Ni**, two peaks were observed. [e]Temperatures at peak positions in ac measurements at zero dc field; the first line is for in-phase ac response and the second line for out-of-phase ac response. For **2Co**, two peaks were observed. Peak positions at high temperature are given here. See the text and Figure 4. [f]Coercive fields. [g]Remnant magnetization. [h]Canting angles; see the text. [i]Fields for spin flop from peak or first turn positions in dM/dH. [j]*g* factors derived from the Curie constants. [k]Estimated from $J/k_B = 3\Theta/[2zS(S+1)]$; see the text.

The temperature dependence of the direct-current (dc) susceptibilities of **1Mn**, **2Co**, and **3Ni**, in plots of χT vs T, measured under fields of 100 Oe and 10 kOe, is shown in Figure 2a. These materials mainly displayed AF character. Under the applied 100 Oe field, the χT values at 300 K were 4.42, 3.21, and 1.20 cm^3·K/mol for **1Mn**, **2Co**, and **3Ni**, respectively, and these are expected.[40] The χT values decreased gradually from 300 to 50 K. Fitting high-temperature susceptibility data by Curie−Weiss law (Figure S6 in the Supporting Information) afforded Curie constants (C)/Weiss temperatures (Θ) in (cm^3·K/mol)/K: 4.64/−14.3 (**1Mn**), 3.84/−56.1 (**2Co**), and 1.48/−73.4 (**3Ni**). These data are comparable to related metal members in other ammonium metal formate series.[9a,b,10−15] The Landé *g* factors derived from the C values are 2.06, 2.86, and 2.43 for **1Mn**, **2Co**, and **3Ni**, respectively, typical for isotropic Mn^{2+} and anisotropic Co^{2+} and Ni^{2+},[40] and the negative Θ values indicate AF exchange interactions between nearest-neighbor metal ions in the materials, although for **2Co**, depopulation of the higher-energy Kramers doublets ($\pm^3/_2$ and $\pm^5/_2$) for the octahedral Co^{2+} ion in the low-temperature region is possible.[41] Upon further cooling, the χT value of **1Mn** reached a minimum of 1.58 cm^3·K/mol at 9.0 K then a small maximum of 1.69 cm^3·K/mol at 8.5 K, and finally 0.43 cm^3·K/mol at 2 K. For **2Co**, the minimum was 1.04 cm^3·K/mol at 15 K, and then χT rose to a high maximum of 69.3 cm^3·K/mol at 9.0 K and finally decrease

dx.doi.org/10.1021/ic302129m | *Inorg. Chem.* 2012, 51, 13363−13372

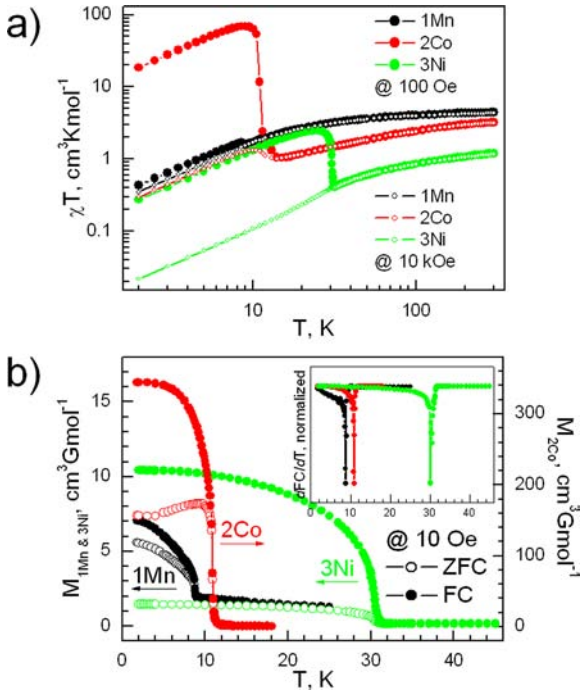

Figure 2. Temperature evolution of dc susceptibility for **1Mn**, **2Co**, and **3Ni**. (a) Plots of χT vs T under 100 Oe field and 10 kOe, in a logarithmic scale for easy observation of the variation of all plots in the low-temperature region. (b) The ZFC/FC plots under 10 Oe field. Inset: dFC/dT data, normalized.

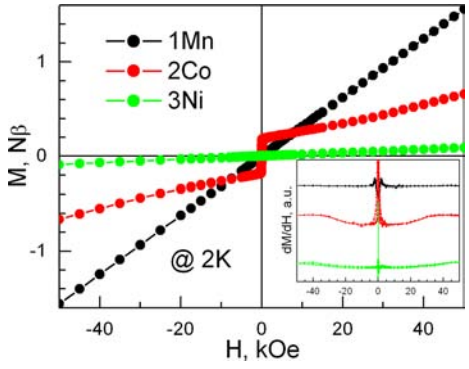

Figure 3. Isothermal magnetization plots of **1Mn**, **2Co**, and **3Ni** at 2 K. Inset: dM/dH plots.

to 18.61 cm^3·K/mol at 2 K. In the case of **3Ni**, the minimum and maximum in χT and the corresponding temperature points were 0.41 cm^3·K/mol/31.6 K and 2.49 cm^3·K/mol/24.0 K, and finally the χT value decreased to 0.27 cm^3·K/mol at 2 K. These results indicate the occurrence of 3D long-range ordering (LRO) of AF with spin canting or WF for the three compounds and the different magnetic anisotropies of the metal ions. Under an applied field of 10 kOe, the χT traces in the high-temperature region almost superposed the traces under 100 Oe field, while in the low-temperature region, the rises after the minima were suppressed for **1Mn** and **3Ni** but still observed for **2Co**. All of these observations characterize the three materials as WFs.

Further magnetic investigation was performed in the low-temperature region, including zero-field-cooled and field-cooled (ZFC/FC) measurements under 10 Oe field (Figure 2b), isothermal magnetization (Figure 3), and ac susceptibility

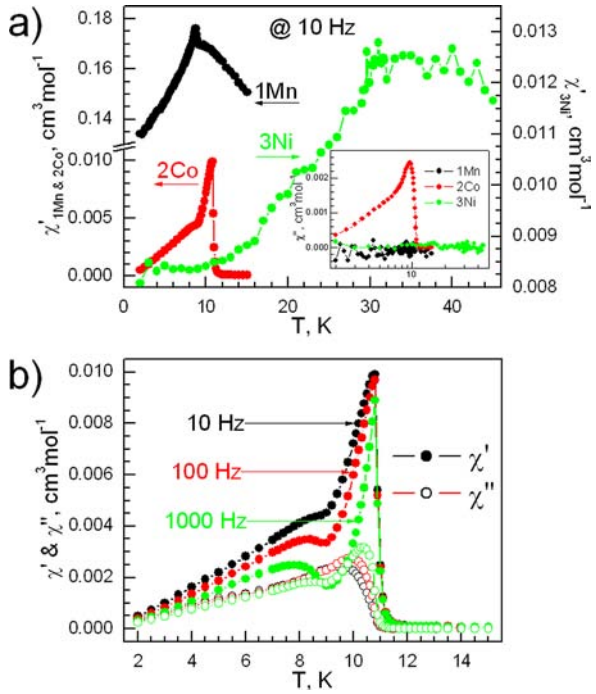

Figure 4. Temperature evolution of the ac susceptibility for **1Mn**, **2Co**, and **3Ni**. (a) Plots of χ' vs T at 10 Hz. Inset: χ'' vs T. (b) Data for **2Co** at 10, 100, and 1000 Hz. Data at 100 and 1000 Hz for **1Mn** and **3Ni** are not given here.

measurements (Figure 4) at frequencies of 10, 100, and 1000 Hz. The bifurcated ZFC/FC traces clearly showed that the irreversibility, locating the 3D LRO of spin-canted AF, and Néel temperatures (T_N's), determined by the negative peak positions on the dFC/dT data (Figure 2b, inset), are 8.8 K (**1Mn**), 10.9 K (**2Co**), and ~30 K (**3Ni**), respectively, although two peaks, 30.5 and 30.0 K for **3Ni**, were resolved. These T_N's are within 1 K of those of the related members of $[NH_4][M(HCOO)_3]$,[10b,c] but for the Co and Ni members, the T_N's are 3−5 K lower than those of the known perovskite or niccolite series.[11,12e,13a,22,23] **1Mn** and **3Ni** possessed very small spontaneous magnetizations of ca. 7 (**1Mn**) and 10 (**3Ni**) cm^3·G/mol, suggesting very small spin-canting angles within these materials. **2Co** had a quite large spontaneous magnetization of ca. 350 cm^3·G/mol, in agreement with the large χT values mentioned above, indicating a large spin-canting angle in **2Co**. **2Co** thus joined the few examples of ammonium transition-metal formates with large spontaneous magnetizations, perovskite $[C(NH_2)_3][Co(HCOO)_3]$[13a] and niccolite $[CH_3NH_2CH_2CH_2NH_2CH_3][Fe_2(HCOO)_6]$.[23a] At 2.0 K, the isothermal magnetizations (Figure 3) revealed typical characterizations of weak ferromagnetism for the three compounds. The coercive fields (H_C)/remanent magnetization (M_R) (Table 3) were 30 Oe/0.0008 Nβ (**1Mn**), 60 Oe/0.11 Nβ (**2Co**), and 1 kOe/0.002 Nβ (**3Ni**), respectively. **2Co** has quite large M_R but is still a soft magnet, while **3Ni** has small M_R but is quite hard. The spin-canting angles α were estimated, by sin $\alpha = M_R/M_S$,[42] as 0.008° (**1Mn**), 1.5° (**2Co**), and 0.5° (**3Ni**), assuming two AF sublattices and $S = {}^5/_2$, ${}^3/_2$, and 1 for **1Mn**, **2Co**, and **3Ni**, respectively. At 50 kOe, the magnetizations were 1.56 Nβ (**1Mn**), 0.66 Nβ (**2Co**), and 0.09 Nβ (**3Ni**), respectively, less than the expected M_S values, confirming the AF LRO again. A spin-flop transition (AF-SP) could be observed, and at 2 K, the fields for spin flop (H_{SP}), estimated by the peak or turning

dx.doi.org/10.1021/ic302129m | Inorg. Chem. 2012, 51, 13363−13372

positions of dM/dH, were 2.0 kOe (**1Mn**), 38 kOe (**2Co**), and probably higher than 40 kOe for **3Ni** (Figure 3, inset).

The temperature evolution traces of the ac susceptibilities (in-phase, χ', and out-of-phase, χ'') under zero dc field for the three compounds are shown in Figure 4. **1Mn** displayed frequency-independent peaks in χ' at 8.7 K, close to T_N by dc measurement, and the χ'' responses were in the noise level. For **2Co**, sharp and frequency-independent peaks in the χ' response were observed at 10.8 K; however, the χ'' peaks are broad and slightly frequency-dependent below T_N, and there were also frequency-dependent shoulder peaks, more pronounced for high frequencies, around 8 K in χ' data, indicating relaxation behavior, with a small parameter of $\phi^{43} = (\Delta T_P/T_P)/\Delta(\log f) \sim 0.05$, where T_P is the peak temperature of χ' and f the ac frequency. Relaxation behaviors are not frequently encountered for ammonium metal formates,[13a] The reason for the relaxation occurring in **2Co** could be domain-wall movement,[44] or chirality-related ac responses as observed in some chiral molecular-based magnets,[45] given the fact that **2Co** is a chiral soft WF with quite large spontaneous magnetization, but this needs further investigation. **3Ni** displayed weak χ' and noisy χ'' responses, and this could be expected given the very small spontaneous magnetization and magnetic hardness of the compound in ordering status. In χ', a turning point around 30 K was observed, indicative of the occurrence of LRO.

The present series has the same framework structure as that of $[NH_4][M(HCOO)_3]$, as discussed before. For this particular framework topology, we could only use the molecular field result, $J/k_B = 3\Theta/[2zS(S + 1)]$,[46] to estimate the M^{II}–M^{II} magnetic couplings through the formato bridge, and the values are −0.40 (**1Mn**), −3.6 K (**2Co**), and −9.2 K (**3Ni**), for $z = 6$ and $S = {}^5/_2$ (**1Mn**), ${}^3/_2$ (**2Co**), and 1 (**3Ni**), respectively, which are comparable to those found in other ammonium metal formate frameworks,[13a,23a] in which the WF is due to the fact that the structures, with the noncentrosymmetric bridges of anti–anti HCOO linking magnetic sites, satisfy the requirement for the occurrence of Dzyaloshinsky–Moriya or the antisymmetric interaction.[47]

Finally, the polycrystalline products of **3Ni**, harvested after 10 days, displayed a sharp rise in their ZFC/FC traces (Figure S2b in the Supporting Information) below 3 K, which was due to the minor impurity of ferrimagnetic $[Ni_3(HCOO)_6]\cdot S$ with a critical temperature of 2.7 K,[9c] and above 3 K, the traces characterized the **3Ni** bulk sample, as just discussed.

CONCLUSION

In conclusion, a new series of ammonium metal formate frameworks of $[HONH_3][M^{II}(HCOO)_3]$ have been successfully synthesized using a simple template of hydroxylammonium $HONH_3^+$ in the presence of bulky triethylammonium in the reaction system, demonstrating the positive templating effect of the small ammonium and negative/none effect of the bulky ammonium. The $HONH_3^+$ with two non-H atoms directed the formation of the dense chiral $4^9\cdot6^6$ metal formate frameworks, similar to the NH_4^+ series but different from the perovskite frameworks with more open void space for accommodating larger monoammoniums of two to four non-H atoms, because of the still small size and its ability to form strong hydrogen bonding. However, the larger size of $HONH_3^+$ than that of NH_4^+ is probably the reason for the simple dielectric properties and no phase transitions within the series, compared to the interesting ferroelectric NH_4^+ series. The three magnetic members of Mn, Co, and Ni show LRO of spin-canted antiferromagnetism, occurring at Néel temperatures of 8.8, 10.9, and 30.5 K, respectively, with small spontaneous magnetizations for the Mn and Ni members but large magnetization for the Co one. While these compounds add a new series of $[AmineH][M(HCOO)_3]$ family, they further demonstrate the templating effect of the ammonium cation, and the chiral magnetic members will be of interest for further magnetooptical studies.

ASSOCIATED CONTENT

Supporting Information

Table S1, Figures S1–S6, and CIF files of crystallography data for the structures in this work. This material is available free of charge via the Internet at http://pubs.acs.org.

AUTHOR INFORMATION

Corresponding Author

*E-mail: zmw@pku.edu.cn (Z.-M.W.), gaosong@pku.edu.cn (S.G.). Fax: 86-10-62751708.

Notes

The authors declare no competing financial interest.

ACKNOWLEDGMENTS

This work was supported by the NSFC (Grants 21171010, 21290170 and 21290171) and the National Basic Research Program of China (Grant 2009CB929403).

REFERENCES

(1) (a) Thematic issue on metal–organic frameworks: Zhou, H.-C.; Long, J. R.; Yaghi, O. M. *Chem. Rev.* **2012**, *112*, 673. (b) Special issue on metal–organic frameworks: Long, J. R.; Yaghi, O. M. *Chem. Soc. Rev.* **2009**, *38*, 1213. (c) Janiak, C.; Vieth, J. K. *New J. Chem.* **2010**, *34*, 2366. (d) Kepert, C. J. *Chem. Commun.* **2006**, 695. (d) Special issue on Reticular Chemistry: O'Keeffe, M.; Yaghi, O. M. *J. Solid State Chem.* **2005**, *178*, 2409. (e) Special issue on Molecular Architectures: Reed, C. A. *Acc. Chem. Res.* **2005**, *38*, 215.

(2) (a) Cheetham, A. K.; Rao, C. N. R. *Science* **2007**, *318*, 58. (b) Rao, C. N. R.; Cheetham, A. K.; Thirumurugan, A. *J. Phys.: Condens. Matter* **2008**, *20*, 083202.

(3) (a) Suh, M. P.; Park, H. J.; Prasad, T. K.; Lim, D.-W. *Chem. Rev.* **2012**, *112*, 782. (b) Meek, S. T.; Greathouse, J. A.; Allendorf, M. D. *Adv. Mater.* **2011**, *23*, 249. (c) Farrusseng, D.; Aguado, S.; Pinel, C. *Angew. Chem., Int. Ed.* **2009**, *48*, 7502. (d) Collins, D. J.; Zhou, H. C. *J. Mater. Chem.* **2007**, *17*, 3154. (e) Li, J.-R.; Sculley, J.; Zhou, H.-C. *Chem. Rev.* **2012**, *112*, 869. (f) Horcajada, P.; Gref, R.; Baati, T.; Allan, P. K.; Maurin, G.; Couvreur, P.; Férey, G.; Morris, R. E.; Serre, C. *Chem. Rev.* **2012**, *112*, 1232. (g) Férey, G. *Chem. Soc. Rev.* **2008**, *37*, 191. (h) Kitagawa, S.; Kitaura, R.; Noro, S. *Angew. Chem., Int. Ed.* **2004**, *43*, 2334.

(4) (a) Wang, C.; Zhang, T.; Lin, W. *Chem. Rev.* **2012**, *112*, 1084. (b) Morris, R. E.; Bu, X. *Nat. Chem.* **2010**, 353. (c) Evans, O. R.; Lin, W. B. *Acc. Chem. Res.* **2002**, *35*, 511. (d) Harbuzaru, B. V.; Corma, A.; Rey, F.; Jordá, J. L.; Ananias, D.; Carlos, L. D.; Rocha, J. *Angew. Chem., Int. Ed.* **2009**, *48*, 6476. (e) Allendorf, M. D.; Bauer, C. A.; Bhaktaa, R. K.; Houka, R. J. T. *Chem. Soc. Rev.* **2009**, *38*, 1330. (f) Chen, B.; Yang, Y.; Zapata, F.; Lin, G.; Qian, G.; Lobkovsky, E. B. *Adv. Mater.* **2007**, *19*, 1693.

(5) (a) Weng, D. F.; Wang, Z. M.; Gao, S. *Chem. Soc. Rev.* **2011**, *40*, 3157. (b) Molecule-based magnets themed issue: Miller, J. S.; Gatteschi, D. *Chem. Soc. Rev.* **2011**, *40*, 3065. (c) Kurmoo, M. *Chem. Soc. Rev.* **2009**, *38*, 1353. (d) Special issue for the forum on Molecular Magnetism: The Role of Inorganic Chemistry: Coronado, E.; Dunbar, K. R. *Inorg. Chem.* **2009**, *48*, 3293. (e) Special issue on crystal engineering in molecular magnetism: Rovira, C.; Veciana, J. *CrystEngComm* **2009**, *11*, 2031. (f) Zhang, W.; Xiong, R.-G. *Chem.*

Rev. **2012**, *112*, 1163. (g) Zhang, W.; Ye, H.-Y.; Xiong, R.-G. *Coord. Chem. Rev.* **2009**, *253*, 2980.
(6) (a) Pardo, E.; Train, C.; Liu, H.; Chamoreau, L.-M.; Dkhil, B.; Boubekeur, K.; Lloret, F.; Nakatani, K.; Tokoro, H.; Ohkoshi, S.-i.; Verdaguer, M. *Angew. Chem., Int. Ed.* **2012**, *51*, 8356. (b) Zhang, W.; Cai, Y.; Xiong, R.-G.; Yoshikawa, H.; Awaga, K. *Angew. Chem., Int. Ed.* **2010**, *49*, 6608. (c) Ohkoshi, S.-i.; Tokoro, H.; Matsuda, T.; Takahashi, H.; Irie, H.; Hashimoto, K. *Angew. Chem., Int. Ed.* **2007**, *46*, 3238.
(7) (a) Train, C.; Gheorghe, R.; Krstic, V.; Chamoreau, L.-M.; Ovanesyan, N. S.; Rikken, G. L. J. A.; Gruselle, M.; Verdagure, M. *Nat. Mater.* **2008**, 729. (b) Train, C.; Gruselle, M.; Verdaguer, M. *Chem. Soc. Rev.* **2011**, *40*, 3297. (c) Inoue, K.; Ohkoshi, S.-I.; Imai, H. In *Magnetism: Molecules to Materials V*; Miller, J. S., Drillon, M., Eds.; Wiley-VCH Verlag GmbH & Co. KGaA: Weinheim, Germany, 2005; Chapter 2. (d) Sato, O.; Tao, J.; Zhang, Y. Z. *Angew. Chem., Int. Ed.* **2007**, *46*, 2152. (e) Sato, O. *Acc. Chem. Res.* **2003**, *36*, 692. (f) Evans, J. S. O.; Bénard, S.; Yu, P.; Clément, R. *Chem. Mater.* **2001**, *13*, 3813.
(8) (a) Dechambenoit, P.; Long, J. R. *Chem. Soc. Rev.* **2011**, *40*, 3249. (b) Maspoch, D.; Ruiz-Molina, D.; Veciana, J. *Chem. Soc. Rev.* **2007**, *36*, 770. (c) Cheng, X.-N.; Zhang, W.-X.; Lin, Y.-Y.; Zheng, Y.-Z.; Chen, X.-M. *Adv. Mater.* **2007**, *19*, 1494. (d) Kaye, S. S.; Choi, H. J.; Long, J. R. *J. Am. Chem. Soc.* **2008**, *130*, 16921. (e) Kurmoo, M.; Kumagai, H.; Chapman, K. W.; Kepert, C. J. *Chem. Commun.* **2005**, 3012. (f) Ohkoshi, S.-I.; Arai, K.-I.; Sato, Y.; Hashimoto, K. *Nat. Mater.* **2004**, *3*, 857.
(9) (a) Wang, Z. M.; Hu, K. L.; Gao, S.; Kobayashi, H. *Adv. Mater.* **2010**, *22*, 1526. (b) Wang, X.-Y.; Wang, Z.-M.; Gao, S. *Chem. Commun.* **2008**, 281. (c) Wang, Z.-M.; Zhang, B.; Zhang, Y.-J.; Liu, T.; Kurmoo, M.; Gao, S.; Kobayashi, H. *Polyhedron* **2007**, *26*, 2207.
(10) (a) Xu, G.-C.; Ma, X.-M.; Zhang, L.; Wang, Z.-M.; Gao, S. *J. Am. Chem. Soc.* **2010**, *132*, 9588. (b) Xu, G.-C.; Zhang, W.; Ma, X.-M.; Chen, Y.-H.; Zhang, L.; Cai, H.-L.; Wang, Z.-M.; Xiong, R.-G.; Gao, S. *J. Am. Chem. Soc.* **2011**, *133*, 14948. (c) Wang, Z. M.; Zhang, B.; Inoue, K.; Fujiwara, H.; Otsuka, T.; Kobayashi, H.; Kurmoo, M. *Inorg, Chem.* **2007**, *46*, 437. (d) Wang, Z. M. *The 5th Japanese–Russian Workshop on Open Shell Compounds and Molecular Spin Devices*, Awaji, Japan, Nov 2011. (e) Ma, X. M. B.Sc. Thesis, Beijing University, Peking, China, 2009. (f) Xu, G. C.; Ma, X. M.; Zhang, L.; Wang, Z. M.; Gao, S. *The 12th International Conference on Molecule-Based Magnetism*, Beijing, China, Oct 2010. (g) Chen, Y. H. B.Sc. Thesis, Beijing University, Peking, China, 2008. (h) Li, W.; Probert, M. R.; Kosa, M.; Bennett, T. D.; Thirumurugan, A.; Burwood, R. P.; Parinello, M.; Howard, J. A. K.; Cheetham, A. K. *J. Am. Chem. Soc.* **2012**, *134*, 11940.
(11) (a) Wang, Z. M.; Zhang, B.; Otsuka, T.; Inoue, K.; Kobayashi, H.; Kurmoo, M. *Dalton Trans.* **2004**, 2209. (b) Shang, R.; Sun, X.; Wang, Z.-M.; Gao, S. *Chem.—Asian J.* **2012**, *7*, 1697.
(12) (a) Fu, D.-W.; Zhang, W.; Cai, H.-L.; Zhang, Y.; Ge, J.-Z.; Xiong, R.-G.; Huang, S. D.; Nakamura, T. *Angew. Chem., Int. Ed.* **2011**, *50*, 11947. (b) Jain, P.; Ramachandran, V.; Clark, R. J.; Zhou, H. D.; Toby, B. H.; Dalal, N. S.; Kroto, H. W.; Cheetham, A. K. *J. Am. Chem. Soc.* **2009**, *131*, 13625. (c) Jain, P.; Dalal, N. S.; Toby, B. H.; Kroto, H. W.; Cheetham, A. K. *J. Am. Chem. Soc.* **2008**, *130*, 10450. (d) Sánchez-Andújar, M.; Presedo, S.; Yáñez-Vilar, S.; Castro-García, S.; Shamir, J.; Señarís-Rodríguez, M. A. *Inorg. Chem.* **2010**, *49*, 1510. (e) Wang, X. Y.; Gan, L.; Zhang, S. W.; Gao, S. *Inorg. Chem.* **2004**, *43*, 4615. (f) Pato-Doldán, B.; Sánchez-Andújar, M.; Gómez-Aguirre, L. C.; Yáñez-Vilar, S.; López-Beceiro, J.; Gracia-Fernández, C.; Haghighirad, A. A.; Ritter, F.; Castro-García, S.; Señarís-Rodríguez, M. A. *Phys. Chem. Chem. Phys.* **2012**, *14*, 8498. (g) Rossin, A.; Ienco, A.; Costantino, F.; Montini, T.; Credico, B. D.; Caporali, M.; Gonsalvi, L.; Fornasiero, P.; Peruzzini, M. *Cryst. Growth Des.* **2008**, *8*, 3302.
(13) (a) Hu, K.-L.; Kurmoo, M.; Wang, Z.-M.; Gao, S. *Chem.—Eur. J.* **2009**, *15*, 12050. (b) Stroppa, A.; Jain, P.; Barone, P.; Marsman, M.; Perez-Mato, J. M.; Cheetham, A. K.; Kroto, H. W.; Picozzi, S. *Angew. Chem., Int. Ed.* **2011**, *50*, 5847.
(14) (a) Zhou, B.; Imai, Y.; Kobayashi, A.; Wang, Z.-M.; Kobayashi, H. *Angew. Chem., Int. Ed.* **2010**, *50*, 11441. (b) Imai, Y.; Zhou, B.; Ito, Y.; Kobayashi, A.; Wang, Z.-M.; Kobayashi, H. *Chem.—Asian J.* **2012**, *7*, 2786.
(15) Rossin, A.; Chierotti, M. R.; Giambastiani, G.; Gobettob, R.; Peruzzini, M. *CrystEngComm* **2012**, *14*, 4454.
(16) (a) Wang, Z. M.; Zhang, B.; Fujiwara, H.; Kobayashi, H.; Kurmoo, M. *Chem. Commun.* **2004**, 416. (b) Zhang, B.; Wang, Z. M.; Kurmoo, M.; Gao, S.; Inoue, K.; Kobayashi, H. *Adv. Funct. Mater.* **2007**, *17*, 577. (c) Dybtsev, D. N.; Chun, H.; Yoon, S. H.; Kim, D.; Kim, K. *J. Am. Chem. Soc.* **2004**, *126*, 32.
(17) (a) Wang, Z. M.; Zhang, Y. J.; Liu, T.; Kurmoo, M.; Gao, S. *Adv. Funct. Mater.* **2007**, *17*, 1523. (b) Viertelhaus, M.; Adler, P.; Clérac, R.; Anson, C. E.; Powell, A. K. *Eur. J. Inorg. Chem.* **2005**, 692.
(18) (a) Wang, Z. M.; Zhang, B.; Kurmoo, M.; Green, M. A.; Fujiwara, H.; Otsuka, T.; Kobayashi, H. *Inorg. Chem.* **2005**, *44*, 1230. (b) Li, K.; Olson, D. H.; Lee, J. Y.; Bi, W. H.; Wu, K.; Yuen, T.; Xu, Q.; Li, J. *Adv. Funct. Mater.* **2008**, *18*, 2205.
(19) Wang, Z. M.; Zhang, Y. J.; Kurmoo, M.; Liu, T.; Vilminot, S.; Zhao, B.; Gao, S. *Aust. J. Chem.* **2006**, *59*, 617.
(20) (a) Rood, J. A.; Noll, B. C.; Henderson, K. W. *Inorg. Chem.* **2006**, *45*, 5521. (b) Mallick, A.; Saha, S.; Pachfule, P.; Roy, S.; Banerjee, R. *Inorg. Chem.* **2011**, *50*, 1392.
(21) (a) Cui, H. B.; Takahashi, K.; Okano, Y.; Kobayashi, H.; Wang, Z. M.; Kobayashi, A. *Angew. Chem., Int. Ed.* **2005**, *44*, 6508. (b) Cui, H. B.; Wang, Z. M.; Takahashi, K.; Okano, Y.; Kobayashi, H.; Kobayashi, A. *J. Am. Chem. Soc.* **2006**, *128*, 15074.
(22) (a) Wang, Z. M.; Gao, S. *The 1st Asian Conference of Coordination Chemistry*, Okazaki, Japan, July 2007. (b) Jiang, Z. C. B.Sc. Thesis, Peking University, Peking, China, 2007. (c) Hu, K.-L. Ph.D. Thesis, Peking University, Peking, China, 2010. (d) Li, M.-Y. Ph.D. Thesis, Peking University, Peking, China, 2011.
(23) (a) Li, M.-Y.; Kurmoo, M.; Wang, Z. M.; Gao, S. *Chem.—Asian J.* **2011**, *6*, 3084. (b) Wang, Z. M.; Zhang, X. Y.; Batten, S. R.; Kurmoo, M.; Gao, S. *Inorg. Chem.* **2007**, *46*, 8439.
(24) (a) Li, M.-Y.; Liu, B.; Wang, B.-W.; Wang, Z.-M.; Gao, S.; Kurmoo, M. *Dalton Trans.* **2011**, *40*, 6038. (b) Liu, B.; Zheng, H.-B; Wang, Z.-M.; Gao, S. *CrystEngComm* **2011**, *13*, 5285. (c) Rossin, A.; Giambastiani, G.; Peruzzini, M.; Sessoli, R. *Inorg. Chem.* **2012**, *51*, 6962.
(25) (a) Hagen, K. S.; Naik, S. G.; Huynh, B. H.; Masello, A.; Christou, G. *J. Am. Chem. Soc.* **2009**, *131*, 7516. (b) Zhao, J.-P.; Hu, B.-W.; Lloret, F.; Tao, J.; Yang, Q.; Zhang, X.-F.; Bu, X.-H. *Inorg. Chem.* **2010**, *49*, 10390.
(26) (a) Ramesh, R. *Nature* **2009**, *461*, 1218. (b) Rogez, G.; Viart, N.; Drillon, M. *Angew. Chem., Int. Ed.* **2010**, *49*, 1921. (c) Akbashev, A. R.; Kaul, A. R. *Russ. Chem. Rev.* **2011**, *80*, 1159.
(27) (a) *COLLECT: data collection software*; Nonius BV: Delft, The Netherlands, 1998. (b) *HKL2000* and *maXus* softwares; University of Glasgow: Scotland, UK, Nonius B.V.: Delft, The Netherlands, and MacScience Co. Ltd.: Yokohama, Japan, 2000. *maXus software*; MacScience Co. Ltd.: Yokohama, Japan, 2000. (c) Blessing, R. H. *Acta Crystallogr.* **1995**, *A51*, 33. (d) Blessing, R. H. *J. Appl. Crystallogr.* **1997**, *30*, 421.
(28) Flack, H. D.; Bernardinelli, G. *Chirality* **2008**, *20*, 681.
(29) Sheldrick, G. M. *SHELX-97, Program for Crystal Structure Determination*; University of Göttingen: Göttingen, Germany, 1997.
(30) Mulay, L. N.; Boudreaux, E. A. *Theory and Applications of Molecular Diamagnetism*; John Wiley & Sons Inc.: New York, 1976.
(31) (a) Nakamoto, K. *Infrared and Raman Spectra of Inorganic and Coordination Compounds*; Wiley: New York, 1986. (b) Williams, D. H.; Fleming, I. *Spectroscopic Method in Organic Chemistry*, 5th ed.; McGraw-Hill Book Co.: Beijing, China, 1998. (c) Stoilova, D.; Koleva, V. *J. Mol. Struct.* **2000**, *553*, 131. (d) Stoilova, D.; Koleva, V. *J. Mol. Struct.* **2001**, *560*, 15.
(32) (a) Yeo, G. A.; Ford, T. A. *J. Mol. Struct.* **1990**, *217*, 307. (b) Withnall, R.; Andrews, L. *J. Phys. Chem.* **1988**, *92*, 2155.
(33) (a) Duan, Z.-M.; Wang, Z.-M.; Gao, S. *Dalton Trans.* **2011**, *40*, 4465. (b) Duan, Z.-M. *Report for postdoctoral research*; Peking University: Peking, China, 2011.

(34) (a) Pabst, A. *Can. Mineral.* **1978**, *16*, 437. (b) Furmanova, N. G.; Soboleva, L. V.; Belov, N. V.; Belyaev, L. M. *Kristallografiya* **1981**, *26*, 1315.
(35) (a) Braga, D.; Grepionia, F.; Novoa, J. J. *Chem. Commun.* **1998**, 1959. (b) Steed, J. W.; Atwood, J. L. *Supramolecular Chemistry*; John Wiley & Sons, Inc.: New York, 2000.
(36) Spek, A. L. *PLATON, A Multipurpose Crystallographic Tool*; Utrecht University: Utrecht, The Netherlands, 2001.
(37) Cotton, F. A.; Wilkinson, G. C.; Murillo, A.; Bochmann, M. *Advanced Inorganic Chemistry*, 6th ed.; Wiley: New York, 1999; p 1304.
(38) (a) This was calculated using *PCMODEL*, version 9.1. See http://www.serenasoft.com. (b) Gille, A. L.; Dutmer, B. C.; Gilbert, T. M. *J. Am. Chem. Soc.* **2009**, *131*, 5714.
(39) Kitaigorodsky, A. I. *Molecular Crystals and Molecules*; Academic Press: New York, 1973; p 18.
(40) Casey, A. T.; Mitra, S. In *Theory and Application of Molecular Paramagnetism*; Mulay, L. N., Boudreaux, E. A., Eds.; Wiley: New York, 1976; pp 183−243.
(41) (a) Lloret, F.; Julve, M.; Cano, J.; Ruiz-García, R.; Pardo, E. *Inorg. Chim. Acta* **2008**, *361*, 3432. (b) Palii, A. V.; Tsukerblat, B. S.; Coronado, E.; Clemente-Juan, J. M.; Borras-Almenar, J. J. *Inorg. Chem.* **2003**, *42*, 2455. (c) Carlin, R. L. *Magnetochemistry*; Springer-Verlag: Berlin, Germany, 1986; pp 65−67. (d) Figgis, B. N.; Lewis, J. *Prog. Inorg. Chem.* **1964**, 37. (e) Figgis, B. N.; Gerloch, M.; Lewis, J.; Mabbs, F. E.; Webb, G. A. *J. Chem. Soc. A* **1968**, 2086.
(42) Kahn, O. *Molecular Magnetism*; Wiley-VCH Publishers: New York, 1993.
(43) Mydosh, J. A. *Spin Glass: an Experimental Introduction*; Taylor & Francis: London, 1993.
(44) Balanda, M. In *Relaxation Phenomena: Liquid Crystals, Magnetic Systems, Polymers, High-T_C Superconductors, Metallic Glass*; Haase, W., Wróbel, S., Eds.; Springer-Verlag: Berlin, Germany, 2003; pp 97−99.
(45) (a) Mito, M.; Iriguchi, K.; Deguchi, H.; Kishine, J.; Kikuchi, K.; Ohsumi, H.; Yoshida, Y.; Inoue, K. *Phys. Rev.* **2009**, *B79*, 012406. (b) Mito, M.; Iriguchi, K.; Deguchi, H.; Kishine, J.; Yoshida, Y.; Inoue, K. *J. Appl. Phys.* **2012**, *111*, 103914.
(46) Carlin, R. L. *Magnetochemistry*; Springer-Verlag: Berlin, Germany, 1986.
(47) (a) Dzyaloshinsky, I. *J. Phys. Chem. Solid* **1958**, *4*, 241. (b) Moriya, T. *Phys. Rev.* **1960**, *120*, 91. (c) Moriya, T. In *Magnetism*; Rado, G. T., Suhl, H., Eds.; Academic Press: New York, 1963; Vol. *1*, pp 85−124.